# Isomerization of 2,3-Dihydrofuran and 5-Methyl-2,3-dihydrofuran: Quantum Chemical and Kinetics Calculations

**Faina Dubnikova and Assa Lifshitz***

*Department of Physical Chemistry, The Hebrew University, Jerusalem 91904, Israel*

*Received: July 16, 2001; In Final Form: November 6, 2001*

Density functional theory calculations were carried out to evaluate the potential energy surfaces of the unimolecular isomerizations of 2,3-dihydrofuran and 5-methyl-2,3-dihydrofuran and the interisomerization between the isomerization products. Equilibrium and transition state structures were optimized by the Lee−Yang−Parr correlation functional approximation (B3LYP) using the Dunning correlation consistent polarized double $\xi$ basis set. Energy values at critical points were calculated at the QCISD(T) level of the theory. Isomerization rate constants were calculated using transition state theory and were compared with the experimental results. The agreement between the calculated and the experimental rate constants are in most cases very good.

## I. Introduction

The five-membered furan ring appears in three levels of saturation: furan, dihydrofuran, and tetrahydrofuran. Whereas furan[1−4] and tetrahydrofuran[5] are very stable kinetically, the two isomers of dihydrofuran are relatively unstable.[6−11] Both react and decompose at much lower temperatures than the completely saturated and unsaturated compounds. The main thermal reaction of 2,5-dihydrofuran is $H_2$ elimination from the 2 and 5 positions in the ring to form furan.[6−9] In 2,3-dihydrofuran, the furan ring opens and isomerization products are formed.[10,11] Both isomers undergo very slow fragmentation. The extent of fragmentation compared to isomerization in 2,3-dihydrofuran can be seen in Figure 1.

The isomerization products of 2,3-dihydrofuran are propenyl aldehyde and cyclopropanecarboxaldehyde,[10] and the products of 5-methyl-2,3-dihydrofuran are methyl cyclopropyl ketone and methyl propenyl ketone.[11]

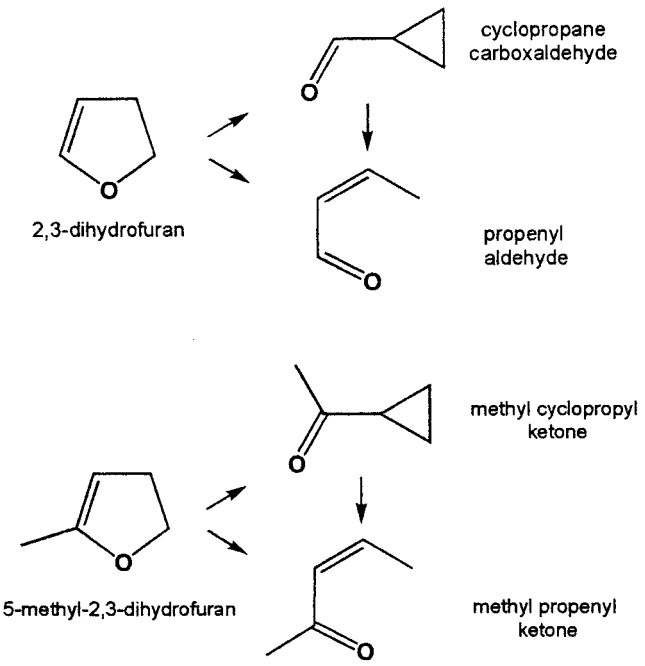


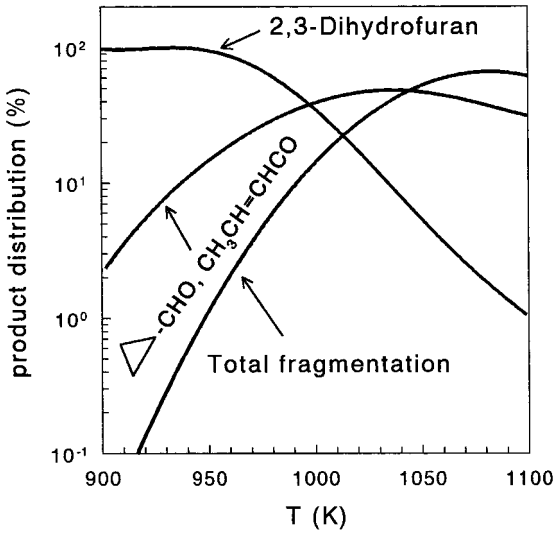


**Figure 1.** Product distribution in the decomposition of 2,3-dihydrofuran. The isomerization reactions are much faster than the total fragmentation at the beginning. As the temperature increases the fragment concentration increases and exceeds the isomer concentrations at 1100 K.

It is of interest to perform quantum chemical calculations and to compare the results of the calculations to the experimental findings. The data available on the isomerization of 5-methyl-2,3-dihydrofuran are considerably more comprehensive and form a much better basis for comparison of the calculations with the experiment than 2,3-dihydrofuran does. We have therefore calculated isomerization rate constants for the two molecules. We present here quantum chemical calculations of the reaction pathways of these compounds and compare the calculations with the experimental results obtained with the single pulse shock tube technique.

## II. Computational Details

We used the Becke three-parameter hybrid method[12] with Lee−Yang−Parr correlation functional approximation (B3LYP)[13] and the Dunning correlation consistent polarized valence double $\xi$ (cc-pVDZ) basis set.[14] Structure optimization of the reactants

10.1021/jp012714h CCC: $22.00 
Published on Web 01/22/2002

**TABLE 1: Structural Parameters of the Species Involved in the Reaction 2,3-Dihydrofuran → Cyclopropanecarboxaldehyde (CPCA) and 5-Methyl-2,3-dihydrofuran → Methyl Cyclopropyl Ketone (MCPK) Calculated at the B3LYP/cc-pVDZ Level of Theory**

| parameter[a,b] | 2,3-dihydrofuran | TS1 | CPCA | 5-methyl-2,3-dihydrofuran | TS5 | MCPK |
|---|---|---|---|---|---|---|
| *r*-O(1)−C(2) | 1.454 | 2.649 | 2.962 | 1.450 | 2.578 | 2.922 |
| *r*-C(2)−C(3) | 1.548 | 1.481 | 1.489 | 1.546 | 1.481 | 1.492 |
| *r*-C(3)−C(4) | 1.516 | 1.502 | 1.530 | 1.513 | 1.499 | 1.526 |
| *r*-C(4)−C(5) | 1.337 | 1.419 | 1.485 | 1.341 | 1.427 | 1.497 |
| *r*-C(5)−O(1) | 1.367 | 1.242 | 1.214 | 1.376 | 1.247 | 1.219 |
| *r*-C(2)−C(4) | 2.367 | 2.452 | 1.530 | 2.358 | 2.462 | 1.526 |
| *r*-C(2)−H(1) | 1.104 | 1.092 | 1.092 | 1.104 | 1.091 | 1.092 |
| *r*-C(2)−H(2) | 1.100 | 1.091 | 1.092 | 1.100 | 1.091 | 1.092 |
| *r*-C(3)−H(3) | 1.106 | 1.109 | 1.092 | 1.107 | 1.110 | 1.092 |
| *r*-C(3)−H(4) | 1.103 | 1.106 | 1.092 | 1.103 | 1.107 | 1.092 |
| *r*-C(5)−C(6) | | | | 1.490 | 1.524 | 1.516 |
| ∠C(2)C(3)C(4) | 101.16 | 110.57 | 60.88 | 101.16 | 111.42 | 60.75 |
| ∠C(3)C(4)C(5) | 108.34 | 120.00 | 117.16 | 108.34 | 119.58 | 117.13 |
| ∠C(4)C(5)O(1) | 115.53 | 125.30 | 124.09 | 115.58 | 122.23 | 121.46 |
| ∠C(2)C(4)C(3) | 39.93 | 34.43 | 58.23 | 39.92 | 34.04 | 61.53 |
| ∠C(5)O(1)C(2) | 106.38 | 87.31 | 59.70 | 106.38 | 90.61 | 58.50 |

[a] Distances are in Angstrom units. [b] The atom numbering is shown in Figure 2.

and products was done using the Berny geometry optimization algorithm.[15] For determining transition state structures, we used the combined synchronous transit-guided quasi-Newton (STQN) method.[16] The higher level calculations were then made using these geometries.

All the calculations were performed without symmetry restrictions. Vibrational analyses were done at the same level of theory to characterize the optimized structures as local minima or transition states. Calculated vibrational frequencies and entropies (at B3LYP level) were used to evaluate preexponential factors of the reactions under consideration. All the calculated frequencies, the zero point energies, and the thermal energies are of harmonic oscillators. The zero-point energies were scaled by the ZPE scaling factor of 0.9806, and the entropies were scaled by the entropy-scaling factor of 1.0015.[17] The calculations of the intrinsic reaction coordinate (IRC), to check whether the transition states under consideration connect the expected reactants and products, were done at the B3LYP level of theory with the same basis set as was used for the stationary point optimization. These calculations were done on all the transition states.

The points on the potential energy surfaces, having a biradical character were located by the unrestricted uB3LYP method using guess wave function with the destructive $\alpha-\beta$ and spatial symmetry. We used an open shell singlet approximation for the biradical structures. It should be mentioned that numerous recent studies indicate that the spin-unrestricted B3LYP method for geometry optimization of biradical transition states and intermediates, and for energy barriers on the surface, provided data that were in a reasonable agreement with the results of the multireference or multiconfigurational calculations and the corresponding experimental data.[18−20]

Each optimized B3LYP structure was recalculated at a single-point quadratic CI calculations, including single and double excitations with a triple contribution to the energy−QCISD-(T).[21] All of the reported relative energies include zero-point energy correction (ZPE).

The DFT and QCISD(T) computations were carried out using the Gaussian-98 program package[22] and were done on a DEC Alpha XP1000 1/500 professional workstation.

### III. Results of the Quantum Chemical Calculations

**A. 2,3-Dihydrofuran.** *1. Formation of Cyclopropanecarboxaldehyde.* The potential energy surface of 2,3-dihydrofuran → cyclopropanecarboxaldehyde isomerization is shown in Figure 2. Selected structural parameters of the species on the surface are shown in Table 1 and the energetics, both at B3LYP/cc-pVDZ and QCISD(T)/cc-pVDZ//B3LYP/cc-pVDZ levels of theory, are shown in Table 2.

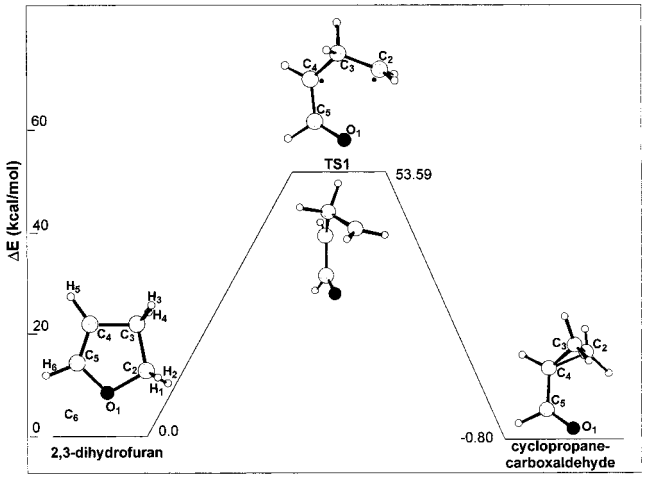


**Figure 2.** Potential energy profile of 2,3-dihydrofuran → cyclopropanecarboxaldehyde isomerization. The transition state TS1 is an open shell singlet. Relative energies (in kcal/mol) are calculated at QCISD-(T)//B3LYP/cc-pVDZ level of theory. Several structural parameters are shown in Table 1.

The surface contains a single transition state TS1, which means that the isomerization proceeds via a concerted mechanism. The atom movement in the normal mode of the imaginary frequency in the transition state indicates that the reaction coordinate is a O(1)−C(2) stretch simultaneously with a conrotatory double rotation of the two methylene groups: the terminal C(2)H(1)H(2) and the central C(3)H(3)H(4). As a result of this rotation the O(1)−C(2) bond is broken and a C(2)−C(4) bond is formed. The distance O(1)−C(2) increases from 1.454 Å in the reactant to 2.649 Å in TS1. C(2)−C(4) decreases from 2.452 Å in the transition state to 1.530 Å in the product. The transition state is an open shell singlet ($\langle S^2\rangle = 0.73$), where the unpaired electrons are distributed on C(2) and C(4). Although the distance between these two carbon atoms in the transition state is still large, the rotation of the two methylene groups and the interaction between the free electron density on the two carbon atoms facilitate the formation of a new C(2)−C(4) bond toward the production of a cyclopropane ring. In the

**TABLE 2: Total Energies $E_{total}$ (in a.u.), Zero Point Energies[a], Relative Energies $\Delta E$[b], Imaginary Frequencies[c], Entropies[d] and Spin Contamination for the Species on the 2,3-dihydrofuran Isomerization Surfaces, Calculated at B3LYP/cc-pVDZ and QCISD(T)/cc-pVDZ//B3LYP/ cc-pVDZ Computational Levels**

| | B3LYP | | | | | | QCISD(T) | |
|---|---|---|---|---|---|---|---|---|
| species | $E_{total}$ | $\Delta E^b$ | ZPE[a] | $S_{298}$[d] | $\nu^c$ | $\langle S^2\rangle$ | $E_{total}$ | $\Delta E$ |
| 2,3-dihydrofuran isomerizations | | | | | | | | |
| 2,3-dihydrofuran | −231.233996 | 0.00 | 56.72 | 67.57 | | 0.0 | −230.598314 | 0.0 |
| TS1 | −231.148333 | 48.97 | 52.03 | 73.21 | (i-155) | 0.73 | −230.505440 | 53.59 |
| cyclopropanecarboxaldehyde | −231.229804 | 1.45 | 55.54 | 71.85 | | 0.0 | −230.597705 | −0.80 |
| TS2 | −231.135457 | 57.09 | 51.98 | 71.48 | (i-1047) | 0.0 | −230.493133 | 61.26 |
| propenyl aldehyde | −231.242620 | −6.19 | 55.94 | 74.85 | | 0.0 | −230.607797 | −6.73 |
| cyclopropanecarboxaldehyde interisomerization | | | | | | | | |
| cyclopropanecarboxaldehyde | −231.229804 | 0.0 | 55.54 | 71.85 | | 0.0 | −230.597705 | 0.0 |
| TS3 | −231.148143 | 47.37 | 51.67 | 73.82 | (i-102) | 0.83 | −230.506918 | 53.10 |
| INT1 | −231.149925 | 46.45 | 51.86 | 76.16 | | 0.90 | −230.507943 | 52.73 |
| TS4 | −231.141411 | 51.42 | 51.49 | 72.61 | (i-1121) | 0.38 | −230.500718 | 56.81 |
| propenyl aldehyde | −231.242620 | −7.64 | 55.94 | 74.85 | | 0.0 | −230.607797 | −5.91 |

[a] Zero-point energies in kcal/mol. ZPE were scaled by the ZPE scaling factor of 0.9806.[17] [b] Relative energies in kcal/mol. $\Delta E = \Delta E_{total} + \Delta$(ZPE). [c] Imaginary frequencies in $cm^{-1}$ [d] Entropies in cal/(K mol). Entropies were scaled by the entropy scaling factor of 1.0015.[17]

**TABLE 3: Structural Parameters of the Species Involved in the Reaction 2,3-Dihydrofuran → Propenyl Aldehyde and 5-Methyl-2,3-dihydrofuran → Methyl Propenyl Ketone (MPK) Calculated at the B3LYP/cc-pVDZ Level of Theory**

| parameter[a,b] | 2,3-dihydrofuran | TS2 | propenyl aldehyde | 5-methyl-2,3-dihydrofuran | TS6 | MPK |
|---|---|---|---|---|---|---|
| *r*-O(1)−C(2) | 1.454 | 2.422 | 3.049 | 1.450 | 2.366 | 3.175 |
| *r*-C(2)−C(3) | 1.548 | 1.442 | 1.495 | 1.546 | 1.440 | 1.496 |
| *r*-C(3)−C(4) | 1.516 | 1.439 | 1.350 | 1.513 | 1.435 | 1.349 |
| *r*-C(4)−C(5) | 1.337 | 1.410 | 1.479 | 1.341 | 1.418 | 1.490 |
| *r*-C(5)−O(1) | 1.367 | 1.355 | 1.218 | 1.376 | 1.261 | 1.223 |
| *r*-C(5)−C(6) | | | | 1.490 | 1.521 | 1.520 |
| *r*-C(2)−H(1) | 1.104 | 1.089 | 1.095 | 1.104 | 1.085 | 1.094 |
| *r*-C(2)−H(2) | 1.100 | 1.095 | 1.105 | 1.100 | 1.095 | 1.105 |
| *r*-C(3)−H(3) | 1.106 | 1.210 | | 1.106 | 1.223 | |
| *r*-C(2)−H(3) | | 1.564 | 1.095 | | 1.541 | 1.105 |
| *r*-C(3)−H(4) | 1.103 | 1.101 | 1.098 | 1.103 | 1.101 | 1.098 |
| ∠C(2)C(3)C(4) | 101.16 | 117.39 | 127.94 | 101.16 | 116.69 | 128.50 |
| ∠C(3)C(4)C(5) | 108.34 | 113.38 | 126.82 | 108.34 | 113.16 | 126.92 |
| ∠C(4)C(5)O(1) | 115.53 | 125.78 | 126.89 | 115.58 | 123.49 | 124.06 |
| ∠C(5)O(1)C(2) | 106.38 | 90.58 | 83.65 | 106.38 | 92.39 | 86.06 |

[a] Distances are in Angstrom units. [b] The atom numbering is shown in Figure 3.

transition state TS1, the lengths of all the C−C bonds (except C(4)−C(2)) and of the C−O bond are much closer to the equivalent bond lengths in cyclopropanecarboxaldehyde than to the bonds in 2,3-dihydrofuran (Table 1).

The energy barrier of the transition state TS1 calculated at uQCISD(T)//B3LYP/cc-pVDZ level of theory with ZPE correction is 53.59 kcal/mol.

*2. Formation of Propenyl Aldehyde.* As has been mentioned before, propenyl aldehyde can be produced from both 2,3-dihydrofuran (the reactant) and from its isomerization product, cyclopropanecarboxaldehyde.

*(a) 2,3-Dihydrofuran → Propenyl Aldehyde Isomerization.* Figure 3 shows the potential energy surface of the isomerization of 2,3-dihydrofuran to propenyl aldehyde. Selected structural parameters of the species on the surface are shown in Table 3 and the energetics is shown in Table 2. This surface also contains a single transition state (TS2), meaning that the isomerization 2,3-dihydrofuran to propenyl aldehyde proceeds by a concerted mechanism. This transition state is a closed shell singlet. In a Hartree−Fock instability test we did not find any instability, which indicates that there is no biradical character in this transition state. In this case, the reaction coordinate is a combination of two normal modes, 1,2-H-atom shift and conrotatory double rotation of the two methylene groups C(2)H-(1)H(2) and C(3)H(3)H(4). The hydrogen atom H(3) is moving from C(3) to C(2), forming a partial $\sigma$-bond C(2)−H(3) (1.564 Å) already in the transition state. H(3)−C(3) changes from 1.106 Å in 2,3-dihydrofuran to 1.210 Å in the transition state.

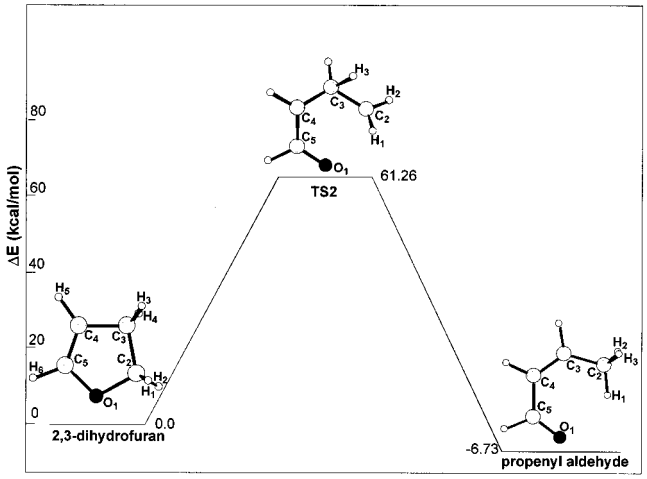


**Figure 3.** Potential energy profile of 2,3-dihydrofuran → propenyl aldehyde isomerization. The transition state TS2 is a closed shell singlet. Relative energies (in kcal/mol) are calculated at QCISD(T)//B3LYP/cc-pVDZ level of theory. Several structural parameters are shown in Table 3.

The energy barrier on this surface is 61.26 kcal/mol at the QCISD(T) level of theory. This value is higher by some 8 kcal/

**TABLE 4: Structural Parameters of the Species Involved in the Reaction Cyclopropanecarboxaldehyde (CPCA) → Propenyl Aldehyde and Methyl Cyclopropyl Ketone (MPCK) → Methyl Propenyl Ketone (MPK) Calculated at the B3LYP/cc-pVDZ Level of Theory**

| parameter[a,b] | CPCA | TS3 | INT1 | TS4 | propenyl aldehyde | MCPK | TS7 | INT2 | TS8 | MPK |
|---|---|---|---|---|---|---|---|---|---|---|
| *r*-C(2)−C(3) | 1.489 | 1.485 | 1.482 | 1.461 | 1.495 | 1.492 | 1.487 | 1.483 | 1.462 | 1.496 |
| *r*-C(2)−C(4) | 1.530 | 2.540 | 2.597 | 2.602 | 2.558 | 1.526 | 2.552 | 2.606 | 2.610 | 2.563 |
| *r*-C(3)−C(4) | 1.530 | 1.494 | 1.487 | 1.446 | 1.350 | 1.526 | 1.492 | 1.488 | 1.446 | 1.349 |
| *r*-C(4)−C(5) | 1.485 | 1.427 | 1.427 | 1.424 | 1.479 | 1.497 | 1.444 | 1.440 | 1.433 | 1.490 |
| *r*-C(5)−O(1) | 1.214 | 1.239 | 1.241 | 1.242 | 1.218 | 1.219 | 1.238 | 1.242 | 1.246 | 1.223 |
| *r*-C(5)−C(6) | | | | | | 1.516 | 1.524 | 1.525 | 1.524 | 1.520 |
| *r*-C(2)−H(1) | 1.092 | 1.090 | 1.089 | 1.089 | 1.095 | 1.092 | 1.090 | 1.087 | 1.088 | 1.094 |
| *r*-C(2)−H(2) | 1.092 | 1.091 | 1.092 | 1.092 | 1.105 | 1.092 | 1.091 | 1.092 | 1.092 | 1.105 |
| *r*-C(3)−H(3) | 1.092 | 1.114 | 1.116 | 1.168 | | 1.092 | 1.114 | 1.116 | 1.167 | |
| *r*-C(3)−H(4) | 1.092 | 1.110 | 1.116 | 1.099 | 1.095 | 1.092 | 1.112 | 1.116 | 1.099 | 1.098 |
| *r*-C(2)−H(3) | | | | 1.695 | 1.105 | | | | 1.698 | 1.105 |
| ∠C(2)C(3)C(4) | 60.88 | 117.01 | 121.98 | 127.02 | 127.94 | 101.16 | 117.85 | 122.64 | 127.75 | 128.50 |
| ∠C(3)C(4)C(5) | 117.16 | 123.97 | 127.28 | 122.99 | 126.82 | 108.34 | 124.29 | 127.40 | 122.98 | 126.92 |
| ∠C(4)C(5)O(1) | 124.09 | 125.14 | 125.36 | 124.92 | 126.89 | 115.58 | 122.22 | 122.63 | 122.24 | 124.06 |

[a] Distances are in Angstrom units. [b] The atom numbering is shown in Figure 4.

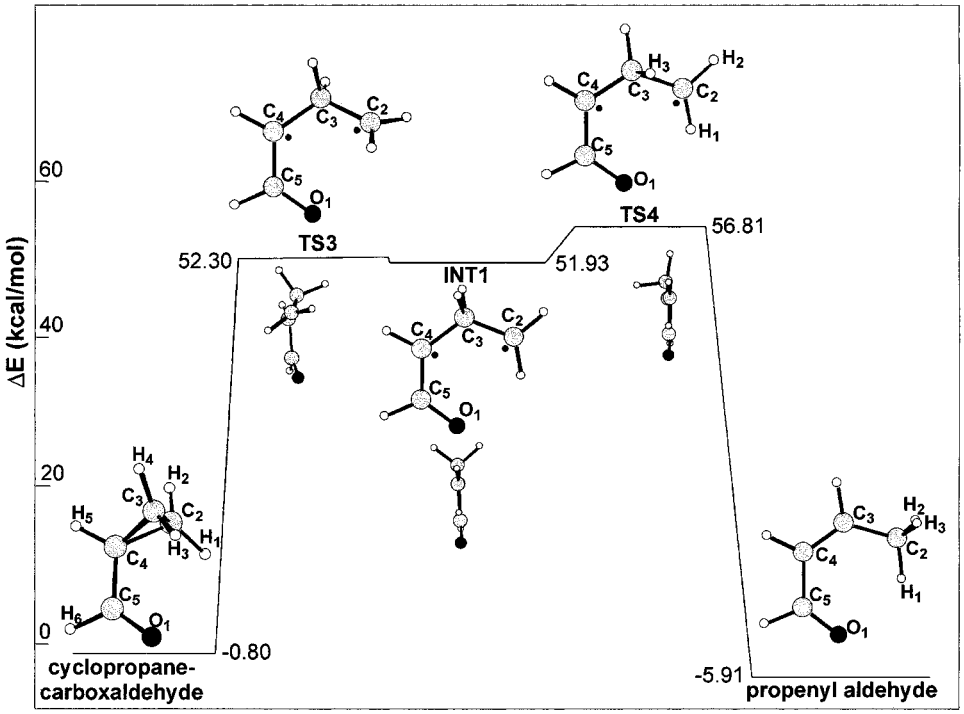


**Figure 4.** Potential energy profile of cyclopropanecarboxaldehyde → propenyl aldehyde interisomerization. The surface contains one intermediate INT1 and two transition states TS3 and TS4. The two transition states and the intermediate are open shell singlets. Relative energies (in kcal/mol) are calculated at QCISD(T)//B3LYP/cc-pVDZ level of theory. Several structural parameters are shown in Table 4.

mol than the 2,3-dihydrofuran → cyclopropanecarboxaldehyde isomerization barrier. This fact can be attributed to an additional 1,2-H-atom shift, which does not exist in the latter.

*(b) Cyclopropanecarboxaldehyde → Propenyl Aldehyde Isomerization.* This reaction proceeds via a stepwise mechanism similar to the cyclopropanecarbonitrile isomerization to crotonitrile, which has been recently studied.[23] As can be seen in Figure 4, the potential energy surface of the cyclopropanecarboxaldehyde → propenyl aldehyde isomerization involves one intermediate and two transition states. The first stage is the cyclopropane ring opening and formation of −HC═O-substituted trimethylene. The reaction coordinate is a conrotatory motion of the methylene group H(1)C(2)H(2) with respect to the central methylene group H(3)C(3)H(4) and disrotatory motion of the oxygen atom with respect to the central methylene group. In TS3 the C(2)−C(4) bond is practically ruptured; it is 2.540 Å compared to 1.530 Å in cyclopropanecarboxaldehyde (Table 4). This distance in the intermediate INT1 further increases to a value of 2.597 Å. Both TS3 and INT1 are biradicals with a spin contamination of 0.83 and 0.90 respectively (see Table 2). The other C−C bonds and the C−O bond are shorter in both TS3 and INT in comparison with cyclopropanecarboxaldehyde.

The reaction coordinate in the transition state TS4 of second stage in this reaction is 1,2-H-atom shift of H(3) from carbon atom C(3) to the terminal carbon C(2). The distance C(3)−H(3) increases to ∼1.17 Å in TS4, in comparison with the length of the same bond in the intermediate, namely, ∼1.12 Å. The new bond, C(2)−H(3) that begins to form in the transition state TS4 decreases its biradical character from a spin contamination of 0.9 to 0.38.

The energy of the ring opening in cyclopropanecarboxaldehyde is 53.10 kcal/mol at the QCISD(T) level of theory. There is a very little difference between the energy of the transition

**TABLE 5: Total Energies $E_{total}$ (in au), Zero Point Energies[a], Relative Energies $\Delta E$[b], Imaginary Frequencies[c], Entropies,[d] and Spin Contamination for the Species on the Isomerization Surfaces of 2-Methyl-4,5-dihydrofuran Isomerization, Calculated at B3LYP/cc-pVDZ and QCISD(T)/cc-pVDZ//B3LYP/cc-pVDZ Computational Levels**

| | B3LYP | | | | | | QCISD(T) | |
|---|---|---|---|---|---|---|---|---|
| species | $E_{total}$ | $\Delta E^b$ | ZPE[a] | $S_{298}$[d] | $\nu^c$ | $\langle S^2 \rangle$ | $E_{total}$ | $\Delta E$ |
| 5-methyl-2,3-dihydrofuran isomerizations | | | | | | | | |
| 5-methyl-2,3-dihydrofuran | −270.558468 | 0.00 | 73.69 | 76.87 | | 0.0 | −269.806745 | 0.0 |
| TS5 | −270.470736 | 50.36 | 69.00 | 82.46 | (i-206) | 0.73 | −269.711036 | 55.37 |
| methyl cyclopropyl ketone | −270.556434 | 0.28 | 72.70 | 79.77 | | 0.0 | −269.807442 | −1.43 |
| TS6 | −270.457969 | 58.50 | 69.13 | 79.71 | (i-1100) | 0.0 | −269.699263 | 62.89 |
| methyl propenyl ketone | −270.567883 | −7.63 | 71.97 | 83.49 | | 0.0 | −269.816144 | −7.62 |
| Methylcyclopropyl ketone isomerizations | | | | | | | | |
| methyl cyclopropyl ketone | −270.556434 | 0.00 | 72.70 | 79.77 | | 0.0 | −269.807442 | 0.0 |
| TS7 | −270.471015 | 49.40 | 68.49 | 84.29 | (i-106) | 0.93 | −269.713956 | 54.46 |
| INT2 | −270.472584 | 48.53 | 68.61 | 87.30 | | 0.91 | −269.714282 | 54.35 |
| TS8 | −270.464322 | 53.48 | 68.37 | 82.73 | (i-1117) | 0.38 | −269.707286 | 58.52 |
| methyl propenyl ketone | −270.567883 | −7.91 | 71.97 | 83.49 | | 0.0 | −269.816144 | −6.19 |

[a] Zero-point energies in kcal/mol. ZPE were scaled by the ZPE scaling factor of 0.9806.[17] [b] Relative energies in kcal/mol. $\Delta E = \Delta E_{total} + \Delta(ZPE)$. [c] Imaginary frequencies in $cm^{-1}$ [d] Entropies in cal/(K mol). Entropies were scaled by the entropy scaling factor of 1.0015.[17]

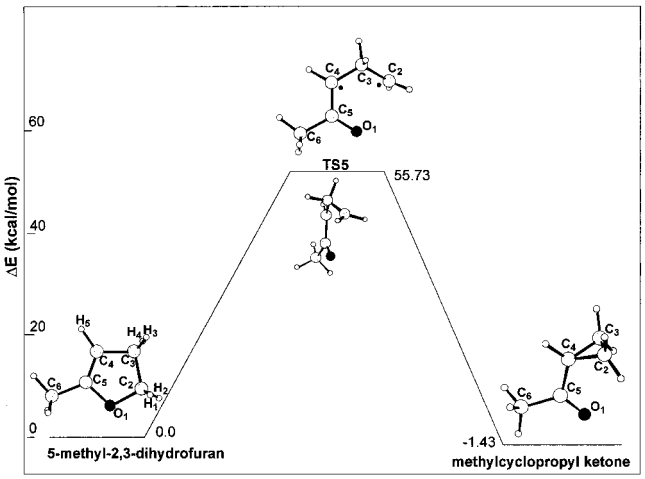


**Figure 5.** Potential energy profile of 5-methyl-2,3-dihydrofuran → methyl cyclopropyl ketone isomerization. The transition state is very similar to the one on the 2,3-dihydrofuran → cyclopropanecarboxaldehyde surface (see Figure 2). Relative energies (in kcal/mol) are calculated at the QCISD(T)//B3LYP/cc-pVDZ level of theory. Several structural parameters are shown in Table 1.

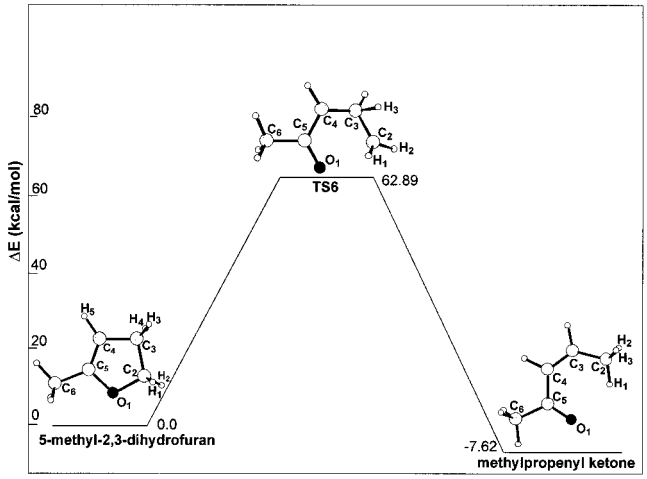


**Figure 6.** Potential energy profile of 5-methyl-2,3-dihydrofuran → methyl propenyl ketone isomerization. The transition state is very similar to the one on the 2,3-dihydrofuran → propenyl aldehyde surface (see Figure 3). Relative energies (in kcal/mol) are calculated at QCISD(T)//B3LYP/cc-pVDZ level of theory. Several structural parameters are shown in Table 3.

state TS3 and the energy of the intermediate INT1. Such a shallow potential energy surface was obtained also in cyclopropanecarbonitrile isomerizations.[23] This is characteristic to small ring rearrangements.[24,25] The barrier of the second stage of the cyclopropanecarboxaldehyde → propenyl aldehyde process relative to the reactant is 56.81 kcal/mol. The barrier from the intermediate INT1 to propenyl aldehyde, which is practically a 1,2-H-atom shift, is 4.08 kcal/mol. The energy barrier for production of propenyl aldehyde from cyclopropanecarboxaldehyde is about 4.5 kcal/mol lower than the barrier for its production directly from 2,3-dihydrofuran.

**B. 5-Methyl-2,3-dihydrofuran.** The isomerization pathways of 5-methyl-2,3-dihydrofuran are very similar to those of 2,3-dihydrofuran, which have been discussed already in detail. We shall therefore not elaborate again on the description of the pathways, only present the results of the calculations.

Figure 5 shows the potential energy surface of the isomerization reaction 5-methyl-2,3-dihydrofuran → methyl cyclopropyl ketone. Figure 6 shows the conversion of 5-methyl-2,3-dihydrofuran to methyl propenyl ketone and Figure 7 shows the interisomerization between the two isomerization products, namely, methyl cyclopropyl ketone → methyl propenyl ketone. As can be seen, all the three surfaces are almost identical to the surfaces describing 2,3-dihydrofuran and its two isomerization products. Selected structural parameters of the species on the potential energy surfaces are added to Tables 1, 3, and 4, and the energetics both at B3LYP/cc-pVDZ and QCISD(T)//B3LYP/cc-pVDZ level of theory are shown in Table 5. The variations in the structural parameters of the species on the 5-methyl-2,3-dihydrofuran potential energy surface, going from the reactants, are very similar to what has been found in 2,3-dihydrofuran. The energetics of the reactions of methyl substituted 2,3-dihydrofuran is also very similar to that of 2,3-dihydrofuran. The differences do not exceed 2 kcal/mol.

## IV. Rate Constant Calculations

To evaluate the high-pressure limit first-order rate constants from the quantum chemical calculations, the relation

$$k_\infty = \Gamma(T)\sigma(kT/h)\exp(\Delta S^{\#}/R)\exp(-\Delta H^{\#}/RT) \qquad (1)$$

was used,[26,27] where $h$ is Planck's constant, $k$ is the Boltzmann factor, $\sigma$ is the degeneracy of the reaction coordinate, $\Delta H^{\#}$ and $\Delta S^{\#}$ are the temperature dependent enthalpy and entropy of activation, respectively, and $\Gamma(T)$ is the tunneling correction.

**TABLE 6: Kinetic and Thermodynamic Parameters for 2,3-Dihydrofuran and 5-Methyl-2,3-dihydrofuran Isomerizations**

| | reaction | $\sigma^a$ | $\Delta S^{\#b}$ | $E_a{}^c$ | $\Delta S°_{\text{reaction}}{}^d$ | $\Delta H°_{\text{reaction}}{}^e$ |
|---|---|---|---|---|---|---|
| 1 | 2,3-dihydrofuran → cyclopropanecarboxaldehyde | 1 | 5.64 | 53.59 | 4.28 | −0.80 |
| 2 | 2,3-dihydrofuran → propenyl aldehyde | 2 | 3.91 | 61.26 | 7.28 | −6.73 |
| 3 | cyclopropanecarboxaldehyde → INT1 | 2 | 1.97 | 53.10 | 4.31 | 52.73 |
| 4 | INT1→ propenyl aldehyde | 2 | −3.55 | 4.08 | −1.31 | −62.72 |
| 3+4 | cyclopropanecarboxaldehyde → propenyl aldehyde | 4 | 0.76 | 56.81 | 3.00 | −5.91 |
| 5 | 5-methyl-2,3-dihydrofuran → methyl cyclopropyl ketone | 1 | 5.59 | 55.37 | 2.90 | −1.43 |
| 6 | 5-methyl-2,3-dihydrofuran → methyl propenyl ketone | 2 | 2.82 | 62.89 | 6.62 | −7.62 |
| 7 | methyl cyclopropyl ketone → INT2 | 2 | 4.52 | 54.46 | 7.53 | 54.35 |
| 8 | INT2 → methyl propenyl ketone | 2 | −4.57 | 4.17 | −3.81 | −64.71 |
| 7+8 | methyl cyclopropyl ketone → methyl propenyl ketone | 4 | 2.96 | 58.52 | 3.72 | −6.19 |

[a] Reaction coordinate degeneracy. [b] Entropy of activation in cal/(K mol) at 298 K. [c] Activation energy in kcal/mol. [d] Entropy of reaction in cal/(K mol) at 298 K. [e] Enthalpy of reaction in kcal/mol at 298 K.

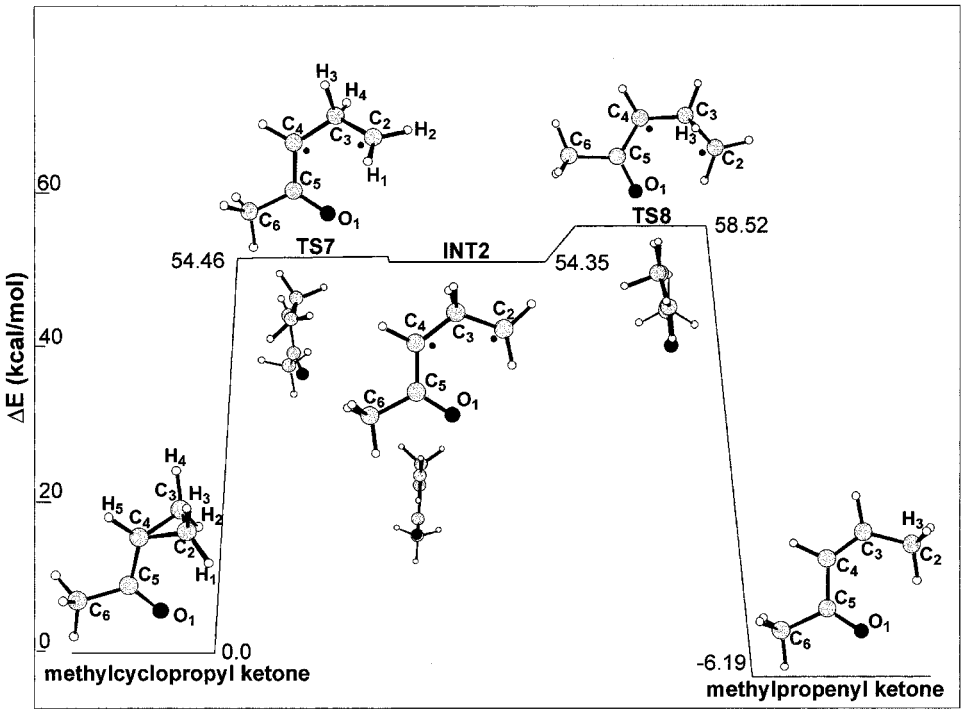


**Figure 7.** Potential energy profile of methyl cyclopropyl ketone → methyl propenyl ketone interisomerization. Similar to the cyclopropanecarboxaldehyde → propenyl aldehyde surface, this surface has also two transitions, TS7 and TS8, and one intermediate, INT2. All these three entities are open shell singlets. Relative energies (in kcal/mol) are calculated at the QCISD(T)//B3LYP/cc-pVDZ level of theory. Several structural parameters are shown in Table 4.

Since we deal with unimolecular reactions, $\Delta H^{\#} = \Delta E^{\#}$, where $\Delta E^{\#}$ is the energy difference between the transition state and the reactant. $\Delta E^{\#}$ is equal to $\Delta E°_{\text{total}} + \Delta E_{\text{thermal}}$, where $\Delta E°_{\text{total}}$ is obtained by taking the difference between the total energies of the transition state and the reactant and $\Delta E_{\text{thermal}}$ is the difference between the thermal energies of these species.

The tunneling effect was estimated using Wigner's inverted harmonic model,[28] where the tunneling effect $\Gamma(T)$ is given by

$$\Gamma(T) = 1 + \frac{1}{24}\left(\frac{hc\bar{\lambda}^{\#}}{kT}\right)^2 \qquad (2)$$

and $\bar{\lambda}^{\#}$ is the imaginary frequency of the reaction coordinate in $cm^{-1}$.[29,30] However, this effect in all the cases that are presented in this report was negligible. Also, RRKM calculations corresponding to the pressure and temperature range of the experiments, with which the calculations were compared, had a negligible effect on the high pressure limit rate constant.

The experimental data available for comparing the calculations with the experiment are considerably more comprehensive for 5-methyl-2,3-dihydrofuran than for 2,3-dihydrofuran, so we will examine the comparison starting from 5-methyl-2,3-dihydrofuran.

**A. 5-Methyl-2,3-dihydrofuran.** *1. 5-Methyl-2,3-dihydrofuran → Methyl Cyclopropyl Ketone.* The rate constant of this isomerization was calculated using eq 1. Kinetic and thermodynamic parameters are given in Table 6. As has been mentioned before, both the tunneling correction (eq 2) and the effect of the RRKM calculations to transfer $k_\infty$ from its high-pressure limit to the pressure used in the experiment (~2 atm) were negligible. Also, since the equilibrium constant of this reaction is high ($K_{eq} = 9.2$ at $T = 950$ K) the back reaction was neglected.

The rate constant was calculated at various temperatures and the values obtained were plotted as log $k$ vs $1/T$. The calculated Arrhenius rate constant obtained from the plot is given by

$$k = 1.90 \times 10^{15} \exp(-58.3 \times 10^3/RT)\ s^{-1}$$

where $R$ is given in units of cal/(K mol). As can be seen in Figure 8, the agreement between the calculated rate constant and the two sets of data at low[31] and at high temperatures[11] is quite good.

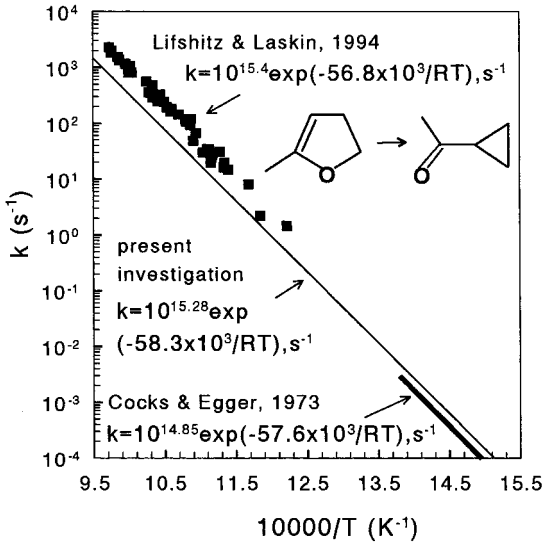


**Figure 8.** Arrhenius plot of the calculated rate constant of 5-methyl-2,3-dihydrofuran → methyl cyclopropyl ketone isomerization. The experimental data at high temperatures are presented as squares on the figure.

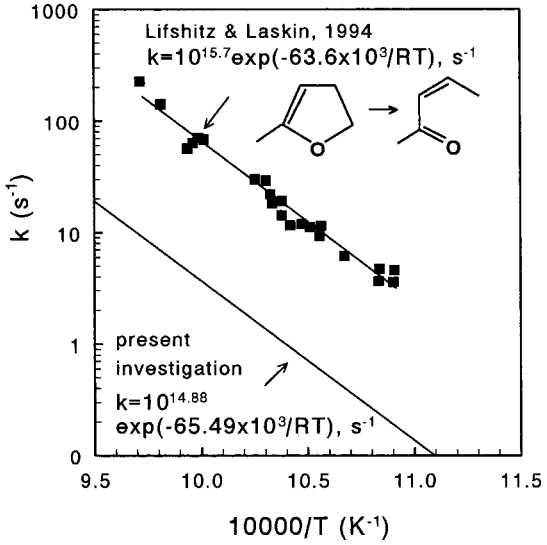


**Figure 9.** Arrhenius plot of the calculated rate constant of 5-methyl-2,3-dihydrofuran → methyl propenyl ketone isomerization. The experimental data at high temperatures are presented as squares on the figure. Experimental data at low temperature are not available. The agreement between the calculated and the experimental rate constant is not very satisfactory.

*2. 5-Methyl-2,3-dihydrofuran → Methyl Propenyl Ketone.* Kinetic and thermodynamic parameters of this reaction are given in Table 6. The rate constants were again calculated at various temperatures using eq 1 and the values obtained were then plotted as log *k* vs 1/*T*. The equilibrium constant of the reaction at 950 K is $K_{eq} = 1583.6$. The rate constant obtained from the Arrhenius plot is given by

$$k = 7.59 \times 10^{14} \exp(-65.49 \times 10^3/RT)\ \mathrm{s}^{-1}$$

Figure 9 shows an Arrhenius plot of the calculated rate constant and the results of recent experimental measurements of the rate constant of this isomerization. As can be seen, the agreement between the two rate constants is not very satisfactory. It amounts to a factor of ∼1/6 in the preexponential factor and 1.9 kcal/mol in the activation energy. At 1000 K it corresponds to about a factor 15 in favor of the experimentally obtained rate constant.

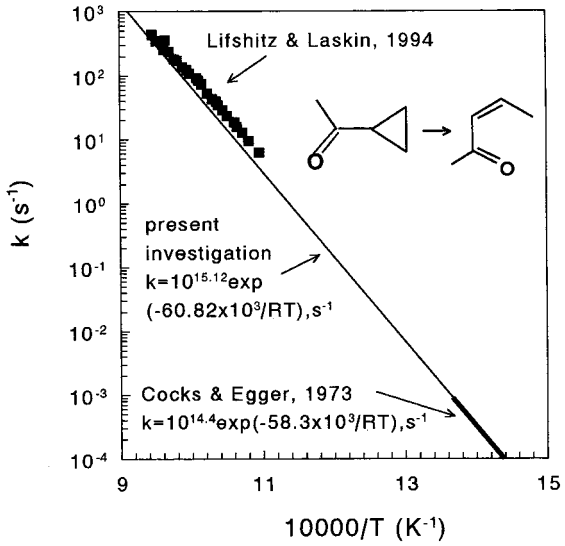


**Figure 10.** Arrhenius plot of the calculated rate constant of methyl cyclopropyl ketone → methyl propenyl ketone interisomerization. The experimental data at high temperatures are presented as squares on the figure.

We do not have a reasonable explanation for this discrepancy. One possibility is an error in the interpretation of the experimental observations. Since the isomerization rate of 5-methyl-2,3-dihydrofuran → methyl propenyl ketone is considerably lower than the rate of the 5-methyl-2,3-dihydrofuran → methyl cyclopropyl ketone isomerization, as has been shown previously, the question was raised whether methyl propenyl ketone is formed also from 5-methyl-2,3-dihydrofuran instead of only from methyl cyclopropyl ketone. This question was addressed by Lifshitz and Laskin[11] who measured experimentally all the three rate constants involved. They reached the conclusion that methyl propenyl ketone is indeed formed from both 5-methyl-2,3-dihydrofuran and methyl cyclopropyl ketone, and it seems that their analysis is correct.

We have calculated the surface of this reaction using an additional quantum chemical method, to verify the calculated rate constant, using QCISD(T)//B3LYP/cc-pVDZ method. Using MP2 (frozen core)/cc-pVDZ, the obtained results ($\Delta S = 1.43$ cal/(K mol) and $\Delta E = 65.29$ kcal/mol) even increased the discrepancy between the calculated and the experimentally measured rate constants. It seems that this issue remains unresolved.

*3. The Interconversion: Methyl Cyclopropyl Ketone → Methyl Propenyl Ketone.* We have examined the possible interconversion between the two isomerization products of 5-methyl-2,3-dihydrofuran. The rate constant for the isomerization was calculated as has been described in the previous section. It was calculated at various temperatures, and the values obtained were plotted as log k vs 1/*T*. The calculated Arrhenius rate constant that was obtained from the plot is given by

$$k = 1.32 \times 10^{15} \exp(-60.82 \times 10^3/RT)\ \mathrm{s}^{-1}$$

where *R* is given in units of cal/(K mol). The equilibrium constant of the reaction at 950 K is $K_{eq} = 172.6$. As can be seen in Figure 10, the calculated rate constant coincides exactly with the extrapolated line of Cocks and Egger[31] who studied the isomerization over the temperature range 670−730 K. It is, however, slightly lower than the experimental points of Lifshitz and Laskin who studied the isomerization at the temperature range 805−1030 K.[11] Altogether the agreement between the

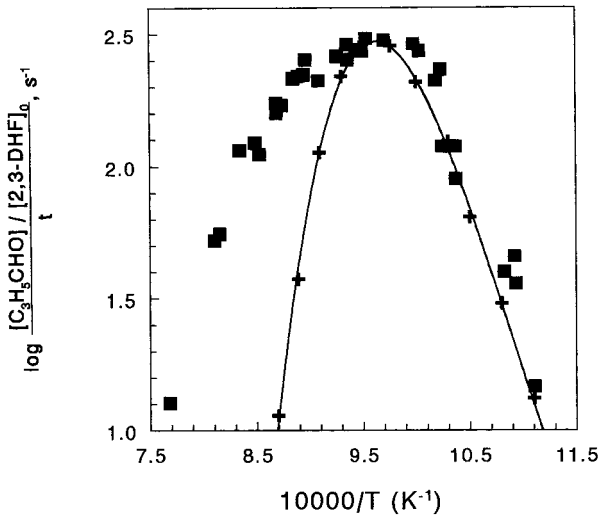


**Figure 11.** A plot of log([cyclopropanecarboxaldehyde]/[2,3-dihydrofuran]$_0$)/$t$ vs 1/$T$. The solid line is the results of the computer modeling that include the three isomerizations calculated at 25 K intervals shown on the figure as +.

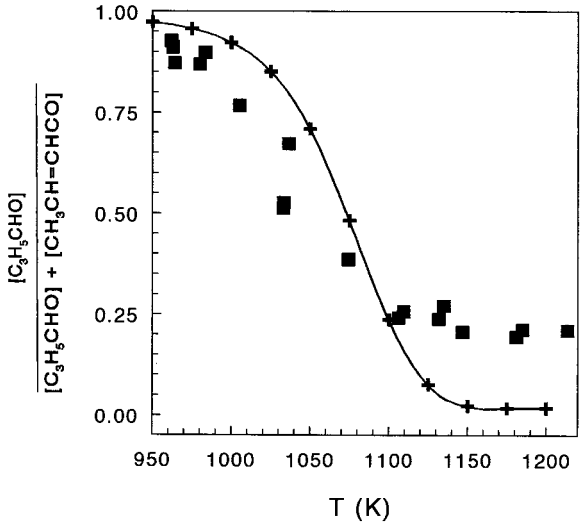


**Figure 12.** A comparison between the calculated and the experimental values of the fraction of cyclopropanecarboxaldehyde to the total isomerization as a function of temperature.

calculated rate constant and the two sets of data at low[31] and at high temperatures[11] is excellent.

**B. 2,3-Dihydrofuran.** As far as we are aware, there is only one study on the thermal decomposition of 2,3-dihydrofuran where the rates of both the isomerization and the fragmentation were measured.[10] However, rate constants were not reported so that modeling calculations had to be made in order to compare the results of the quantum chemical calculations with the experimental observations. We will present our results, starting with rate constant calculations and will then show the comparison between the experimental results and the calculations.

The rate constants for the following three unimolecular reactions were calculated as described in the previous sections for 5-methyl-2,3-dihydrofuran: (1) 2,3-dihydrofuran → cyclopropanecarboxaldehyde; (2) 2,3-dihydrofuran → propenyl aldehyde; (3) cyclopropanecarboxaldehyde → propenyl aldehyde. The values obtained are

$$k_1 = 6.31 \times 10^{14} \exp(-56.30 \times 10^3/RT)\ \mathrm{s}^{-1}$$

$$k_2 = 4.57 \times 10^{14} \exp(-63.57 \times 10^3/RT)\ \mathrm{s}^{-1}$$

$$k_3 = 4.07 \times 10^{14} \exp(-58.88 \times 10^3/RT)\ \mathrm{s}^{-1}$$

Direct measurements of the individual rate constants are not available; however, two other pieces of information are available: log{[cyclopropanecarboxaldehyde]/[2,3-dihydrofuran]$_0$}/$t$ vs 1/$T$ and [cyclopropanecarboxaldehyde]/([cyclopropanecarboxaldehyde]+[propenyl aldehyde]) vs $T$. To calculate these values we performed computer modeling using the above-mentioned three rate constants including the rate constants of the reverse reactions. The results of the modeling are shown in Figures 11 and 12. Figure 11 shows a plot of log([cyclopropanecarboxaldehyde]/[2,3-dihydrofuran]$_0$)/$t$ vs 1/$T$, which at low temperatures resembles an Arrhenius plot of a first-order rate constant (pseudo zero order) for the production of cyclopropanecarboxaldehyde. At higher temperatures, the line bends owing to further isomerization of the product and fragmentation. Since further isomerization of the product takes place to some extent already at low temperatures, the measured slope is smaller than the slope of the true first-order rate constant of the isomerization to cyclopropanecarboxaldehyde. The solid line in Figure 11 is the results of the computer modeling that, as has been mentioned before, took into account all the three isomerizations. As can be seen, the agreement between the calculated and the measured values is very good.

Figure 12 shows a comparison between the calculated and the experimental values of the fraction of cyclopropanecarboxaldehyde relative to the total isomerization as a function of temperature. The squares are the experimental values and the solid line is the results of the modeling calculations. As can be seen, at low temperatures the agreement is reasonable. At high temperatures, 1100 K and higher, the extent of fragmentation exceeds that of isomerization (see Figure 1), so that a comparison cannot be made.

## V. Conclusions

2,3-Dihydrofuran and 5-methyl-2,3-dihydrofuran yield upon isomerization molecules with a cyclopropane structure (cyclopropanecarboxaldehyde and methyl cyclopropyl ketone) as well as open ring structures (propenyl aldehyde and methyl propenyl ketone). The two three-membered ring structures have open shell singlet transition states with no intermediates. The transition states of the production of propenyl aldehyde and methyl propenyl ketone from 2,3-dihydrofuran and 5-methyl-2,3-dihydrofuran have closed shell structures and there are no intermediates on the potential energy surface.

Both propenyl aldehyde and methyl propenyl ketone are formed also by isomerization of the three-membered ring compounds namely, *c*-$C_3H_5CHO$ → $CH_3CH{=}CHCHO$ and *c*-$C_3H_5COCH_3$ → $CH_3CH{=}CHCOCH_3$. The potential energy surfaces of these two isomerizations contain each, two transition states and one intermediate. All the species on the surfaces are open shell singlets.

Rate constants for all the six isomerizations were evaluated from the results of the quantum chemical calculations using transition states theory. The agreement between the calculated rate constant and experimental results in most cases are very good.

**Acknowledgment.** The authors thank the Ministry of Absorption for a fellowship to F.D. in the frame of the Kame'a program.

## References and Notes

(1) Organ, P. P.; Mackie, J. C. *J. Chem. Soc., Faraday Trans.* **1991**, *87*, 815.
(2) Bruinsma, O. S. L.; Tromp, P. J. J.; de Sauvage Nolting, H. J. J.; Moulijn, J. A. *Fuel* **1988**, *67*, 334.
(3) Lifshitz, A.; Bidani, M.; Bidani, S. *J. Phys. Chem.* **1986**, *90*, 5373.
(4) Grela, M. A.; Amorebieta, V. T.; Colussi, A. J. *J. Phys. Chem.* **1985**, *89*, 38.
(5) Lifshitz, A.; Bidani, M.; Bidani, S. *J. Phys. Chem.* **1986**, *90*, 3422.
(6) Lifshitz, A.; Bidani, M. *J. Phys. Chem.* **1986**, *90*, 6011.
(7) James, T. L.; Wellington C. A. *J. Chem. Soc. A* **1968**, 2398.
(8) Wellington C. A.; Walters, W. D. *J. Am. Chem. Soc.* **1961**, *83*, 4888.
(9) Rubin, J. A.; Filseth, S. V. *J. Chem. Educ.* **1969**, *46*, 57.
(10) Lifshitz, A.; Bidani, M.; Bidani, S. *J. Phys. Chem.* **1989**, *93*, 1139.
(11) Lifshitz, A.; Laskin, A. *J. Phys. Chem.* **1994**, *98*, 2341.
(12) Becke, A. D. *J. Chem. Phys.* **1993**, *98*, 5648.
(13) Lee, C.; Yang, W.; Parr, R. G. *Phys. Rev.* **1988**, *B37*, 785.
(14) Dunning, T. H., Jr.; Fabian, J. *Eur. J. Org. Chem* **1999**, 1107.
(15) Schlegel, H. B. *J. Comput. Chem.* **1982**, *3*, 214.
(16) Peng, C.; Schlegel, H. B. *Isr. J. Chem.* **1993**, *33*, 449.
(17) Scott, A. P.; Radom, L. *J. Phys. Chem.* **1996**, *100*, 16502.
(18) Skancke, P. N.; Hrovat, D. A.; Borden, W. T. *J. Phys. Chem.* **1999**, *103*, 4043.
(19) Hess, B. A., Jr.; Eckart, U.; Fabian, J. *J. Am. Chem. Soc.* **1998**, *120*, 12310.
(20) Brinck, T.; Lee, H.-N.; Jonsson, M. *J. Phys. Chem.* **1999**, *103*, 7094.
(21) Pople, J. A.; Head-Gordon, M.; Raghavachari, K. J. *J. Chem Phys.* **1987**, *87*, 5968.
(22) Frisch, M. J.; Trucks, G. W.; Schlegel, H. B.; Scuseria, G. E.; Robb, M. A.; Cheeseman, J. R.; Zakrzewski, V. G.; Montgomery, J. A., Jr.; Stratmann, R. E.; Burant, J. C.; Dapprich, S.; Millam, J. M.; Daniels, A. D.; Kudin, K. N.; Strain, M. C.; Farkas, O.; Tomassi, J.; Barone, V.; Cossi, M.; Cammi, R.; Mennucci, B.; Pomelli, C.; Adamo, C.; Clifford, S.; Oshterski, J.; Petersson, G. A.; Ayala, P. Y.; Cui, Q.; Morokuma, K.; Malick, D. K.; Rabuck, A. D.; Rahavachari, K.; Foresman, J. B.; Cioslowski, J.; Orviz, J. V.; Baboul, A. G.; Stefanov, B. B.; Liu, G.; Liashenko, A.; Piskorz, P.; Komarini, I.; Gomperts, R.; Martin, R. L.; Fox, D. J.; Keith, T.; Al-Laham, M. A.; Peng, C. Y.; Nanayakkara, A.; Gonzalez, C.; Challacombe, M.; Gill, P. M. W.; Johnson, B.; Chen, M. W.; Wong, M. W.; Andres, J. L.; Head-Gordon, M.; Replogle, E. S.; Pople, J. A. GAUSSIAN 98, Revision A.7, Gaussian, Inc.: Pittsburgh, 1998.
(23) Dubnikova, F.; Lifshitz, A. *J. Phys. Chem. A* **1998**, *102*, 5876.
(24) Doubleday, C., Jr.; McIver, J. W.; Page, M. *J. Phys. Chem.* **1988**, *92*, 4367.
(25) Doering, W. von E.; Sachdev, K. *J. Am. Chem. Soc.* **1974**, *96*, 1168.
(26) Eyring, H. *J. Chem. Phys*. **1935**, *3*, 107.
(27) Evans, M. G.; Polanyi, M. *Trans. Faraday Soc*. **1935**, *31*, 875.
(28) Wigner, E. *Z. Physik. Chem.* **1932**, *B19*, 203.
(29) Louis, F.; Gonzales, C. A.; Huie, R.; Kurylo, M. J. *J. Phys. Chem. A* **2000**, *104*, 8773.
(30) George, P.; Glusker, J. P.; Bock, W. *J. Phys. Chem. A* **2000**, *104*, 11347.
(31) Cocks, A. T.; Egger, K. W. *J. Chem. Soc., Perkin Trans.* **1973**, *2*, 199.